JOURNAL OF GEOPHYSICAL RESEARCH, VOL. 92, NO. B5, PAGES 3507-3526, APRIL 10, 1987

TEMPORAL CHANGE IN CODA Q ASSOCIATED WITH THE ROUND VALLEY, CALIFORNIA, EARTHQUAKE OF NOVEMBER 23, 1984

J. Y. Peng,[1] K. Aki,[1] B. Chouet,[2] P. Johnson,[2] W. H. K. Lee,[2] S. Marks,[2] J. T. Newberry,[3] A. S. Ryall,[4] S. W. Stewart,[2] and D. M. Tottingham[2]

Abstract. Seven thousand seismograms of small earthquakes in the Mammoth Lakes-Bishop area were used to measure values of Q from the decay of the earthquake coda. These measurements were compared between events that occurred before and after the Round Valley earthquake (M=5.7). We found that in regions near the main shock epicenter, measurements of coda Q^{-1} for earthquakes that occurred after the main shock were higher than for those earthquakes that occurred prior to the main shock. The opposite behavior was found for regions farther away from the main shock, namely, lower coda Q^{-1} after the main shock than before. Measurements of coda Q^{-1} in the Long Valley caldera, outside of the immediate source region of the earthquake, were higher than in surrounding areas before the main shock, but the difference disappeared after the occurrence of the main shock. This indicates that the temporal variation in coda Q^{-1} is comparable to its spatial variation. The doughnut model (seismicity quiescence surrounded by a zone of activity) which was invoked for explaining the precursory seismicity pattern appears to be similar with the observed coda Q^{-1} variation associated with the Round Valley earthquake. The observed spatial variations in coda Q^{-1} also help to reconcile conflicting results published in previous studies of the coda Q^{-1} precursor.

Introduction

Many researchers have shown in various areas of the world that the coda decay rate of local earthquakes, first discussed by Aki [1969], is a stable parameter which is insensitive to source and receiver locations within an area and reflects the average property of the area containing the sources and receivers. The interpretation of the coda decay rate in terms of apparent attenuation of back-scattering S waves has been largely successful [Kopnichev, 1977; Tsujiura, 1978; Aki, 1980b; Roecker et al., 1982; Sato, 1977, 1984]. The Q^{-1} of S waves thus inferred from the coda decay rate is called "coda Q^{-1}."

Recently, temporal changes of coda Q^{-1} have been reported before and after large earthquakes. Among these reports are (1) a 30% increase in coda Q^{-1} before the 1975 Hawaii (M=7.2) earthquake [Wyss, 1985], (2) a 20% increase in coda Q^{-1} before 3 large earthquakes (M=8.0) in the Kuril-Kamchatka area [Gusev and Lemzikov, 1985], (3) a 30% increase in the value of coda Q^{-1} measured at 6Hz before the Petatlan earthquake (M=7.6) in Mexico (Novelo-Casanova et al., 1985], (4) anomalously high coda Q^{-1} before the eastern Yamanashi earthquake (M=6.0) of 1983 in central Japan [Sato, 1986], (5) a 300% increase in coda Q^{-1} in the 3 years before the Tangshan earthquake (M=7.8) of 1976 and a comparable change for the Haicheng earthquake (M=7.3) of 1975 in China [Jin and Aki, 1986], (6) a 10-20% decrease in coda Q^{-1} during the 2-3 year period before the Misasa earthquake (M=6.2) of October, 1983 in Tottori, Japan [Tsukuda, 1985]. Other evidence suggesting the temporal changes in coda Q^{-1} have also been reported [Chouet, 1979; Jin, 1981; Wilson et al., 1983; Rhea, 1984]. There is a possibility that the coda Q^{-1} changes without an obvious relation to an major earthquake. We probably cannot reject this hypothesis for our case.

In most of the above reported cases, coda Q^{-1} was anomalously high for a period preceding the occurrence of the main shock. In some cases [e.g., Tsukuda, 1985], however, the change was opposite and coda Q^{-1} became higher in the aftershock area after the occurrence of the main shock. The sample regions for the case of Jin and Aki [1986] and others are probably much larger than the aftershock zone because stations for the case of Jin and Aki [1986] are more distant (~100 km) from the epicenter than in the case of Tsukuda [1985], in which two nearby seismic stations are about 10 km from the epicenter of the main shock. Both of these apparently inconsistent patterns may be explained if coda Q^{-1} increases within the aftershock zone but decreases outside of it when the main shock occurs. In this paper, we present evidence that supports the above model using data obtained in the Mammoth Lakes-Bishop area before and after the Round Valley earthquake (M=5.7) of November 23, 1984.

Data

Vertical component seismograms of 70 microearthquakes ($1.5 < M_L < 3.0$) consisting of 60 foreshocks and 10 aftershocks of the Round Valley, California, earthquake of November 23, 1984, each recorded digitally at 100 samples/s at a subset of approximately 100 stations, were processed through the CUSP (California Institute of Technology (Caltech)-U.S. Geological Survey (USGS) Seismic Processing) system [Johnson and Stewart, 1986]. Here we use the words "foreshocks" and "aftershocks" to mean earthquakes that occurred respectively before and after the Round Valley earthquake, noting that they may not be causally related. A description of the data processing employed to evaluate the coda Q^{-1} from this database is given by Lee et al. [1986].

The epicenter of the main shock was at 118.6°W and 37.5°N (Figure 1). Since October 1978, four

[1]Department of Geological Sciences, University of Southern California, Los Angeles.
[2]U.S. Geological Survey, Menlo Park, California.
[3]Sierra Geophysics, Inc., Seattle, Washington.
[4]Center for Seismic Studies, Arlington, Virginia.

Copyright 1987 by the American Geophysical Union.

Paper number 6B6034.
0148-0227/87/006B-6034$05.00

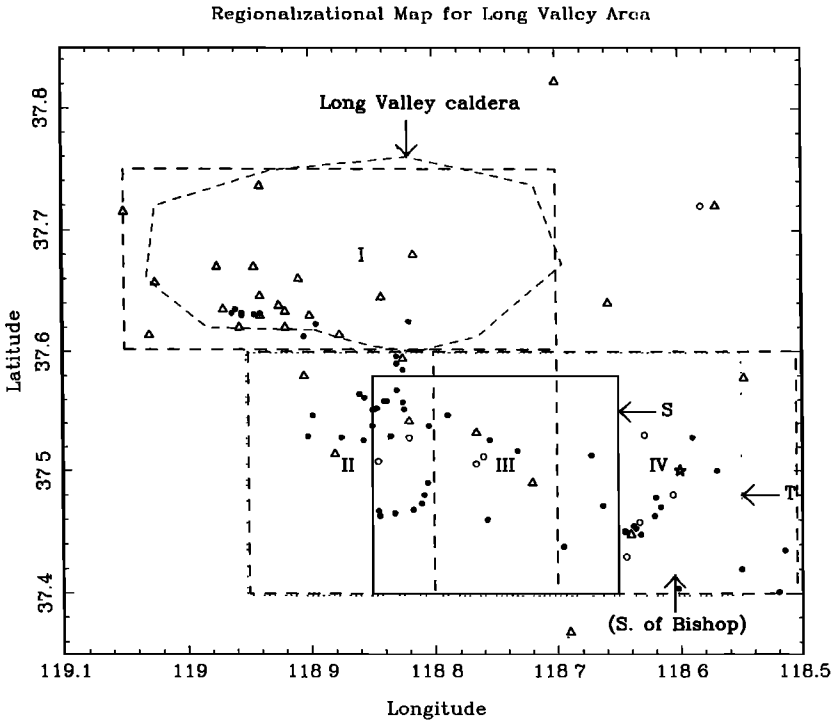

Fig. 1. A map showing seismic stations and the earthquake epicenters. Triangles, recording stations operated by the U.S. Geological Survey and by the University of Nevada; solid circles, foreshock; open circles, aftershocks; star, the Round Valley earthquake (M=5.7) of November 23, 1984. Also shown are six regions used in this study. Regions I, II, III, and IV are depicted by dashed lines. Region S is bounded by the solid line containing most of region III and parts of regions II and IV. Region T includes regions II, III, and most of region IV and is represented by the dotted line. Region I is the Long Valley caldera, and region IV is the north of Bishop area.

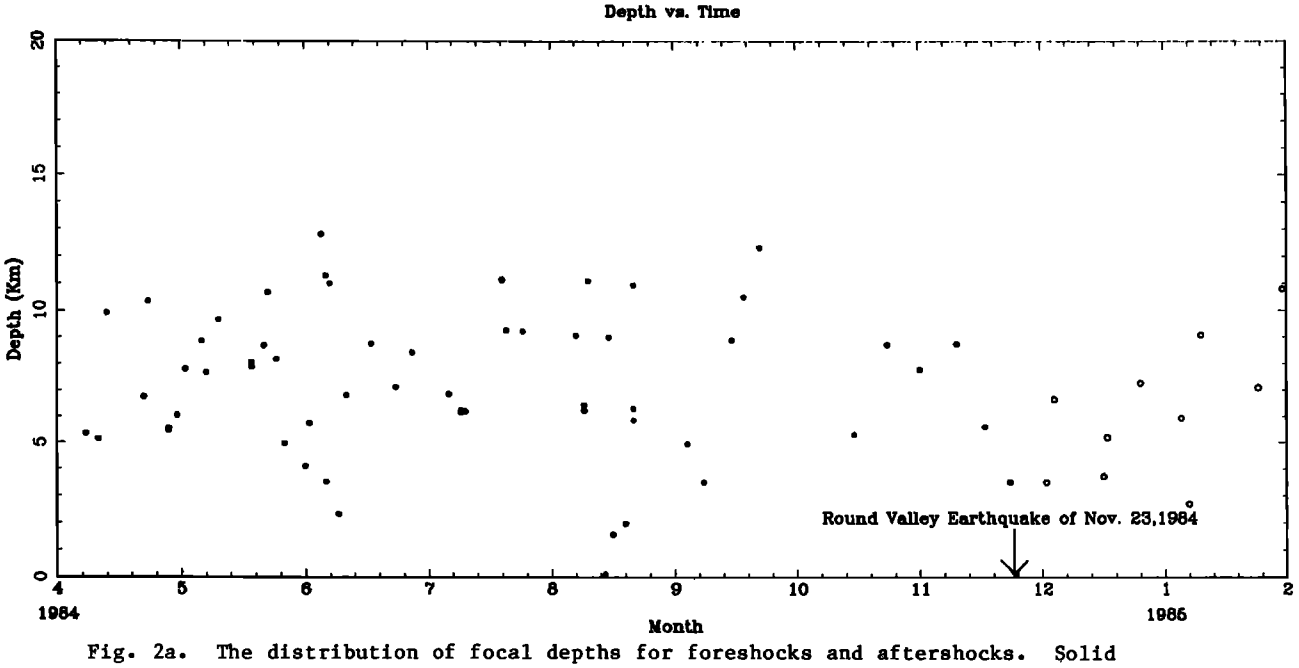

Fig. 2a. The distribution of focal depths for foreshocks and aftershocks. Solid circles represent foreshocks, while open circles represent aftershocks. The arrow indicates the time of the main shock which occurred on November 23, 1984, with magnitude 5.7.

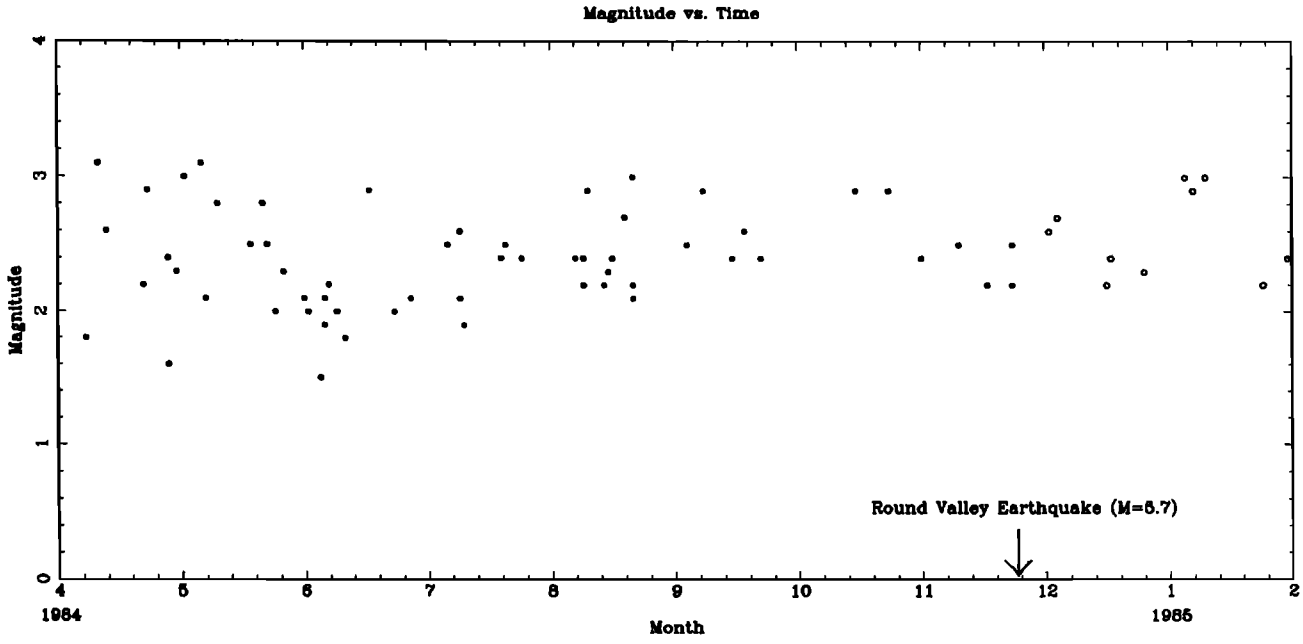

Fig. 2b. The distribution of magnitude versus time for foreshocks (solid circles) and aftershocks (open circles).

earthquakes with magnitude ~ 6 and several earthquake swarms with thousands of smaller events have occurred in the Mammoth Lakes area [Julian and Sipkin, 1985]. Our digital data, however, were collected from April 1984, when the USGS on-line data acquisition systems started full operation, to January 1985. The general distribution of epicenters is similar for foreshocks and aftershocks (Figure 1). The patterns of earthquake occurrences do not show any obviously systematic change for the period covering our data set. Any change in coda Q^{-1}, therefore, is not likely a result of a change in spatial coverage by the coda waves due to a change in earthquake locations. We also found that the distribution of focal depths (0-15 km) did not show any systematic difference between foreshocks and aftershocks (Figure 2a). Moreover, there is not any significant change in magnitude either before or after the main shock (Figure 2b). Table 1 shows that there is not any significant change either in focal depths or magnitudes before and after the main shock when the same statistical test as used in testing for changes in coda Q^{-1} is applied.

Method of Data Analysis

According to Rautian and Khalturin [1978], the observed coda decay rate becomes independent of hypercentral distance for a lapse time (measured from the origin time) more than twice the travel time of direct S waves. In the present paper we have chosen two lapse time windows for the determinations of coda Q^{-1}, namely, 20-45 s and 30-60 s, which roughly correspond to the volume sampled by the single back-scattered waves within the radius of about 65 and 90 km from the midpoint of station and epicenter respectively. We did screen the data to insure that codas waves arriving earlier than twice the S travel time were excluded.

Following Aki and Chouet [1975], the coda power spectrum $P(\omega|t)$ averaged over a frequency band centered at frequency ω and time t (measured from the origin time) is expressed as

$$P(\omega|t) = C(\omega)t^{-m} e^{-\frac{\omega t}{Q_c}} \qquad (1)$$

where $C(\omega)$ represents the coda source factor at the centered frequency ω, m is a constant that depends on geometrical spreading (m=2 for body waves), and Q_c is the quality factor that we wish to determine. Recently, Frankel and Clayton [1986] have questioned the validity of the single-scattering model which is assumed for deriving equation (1). If the single-scattering model is not applicable to the coda, the coda Q derived by equation (1) should not be equal to the Q of S waves. Observations, however, have consistently shown that both the coda Q and Q of S waves have very similar frequency dependence and regional variation for 1-25 Hz [Wu, 1984, Appendix A]. Recent work on Lg by Campillo et al. [1985] shows the frequency dependence

TABLE 1. Means of Focal Depths and Magnitudes, Number of Events Used to Calculate Standard Error of the Mean Before and After the Main Shock

	Foreshock			Aftershock		
	Mean	Number of Events	SEM	Mean	Number of Events	SEM
Focal Depth	7.23	59	0.39	6.20	10	0.81
Magnitude	2.38	59	0.05	2.57	10	0.10

Difference between shoreshocks and aftershocks is not significant. SEM, standard error of the mean.

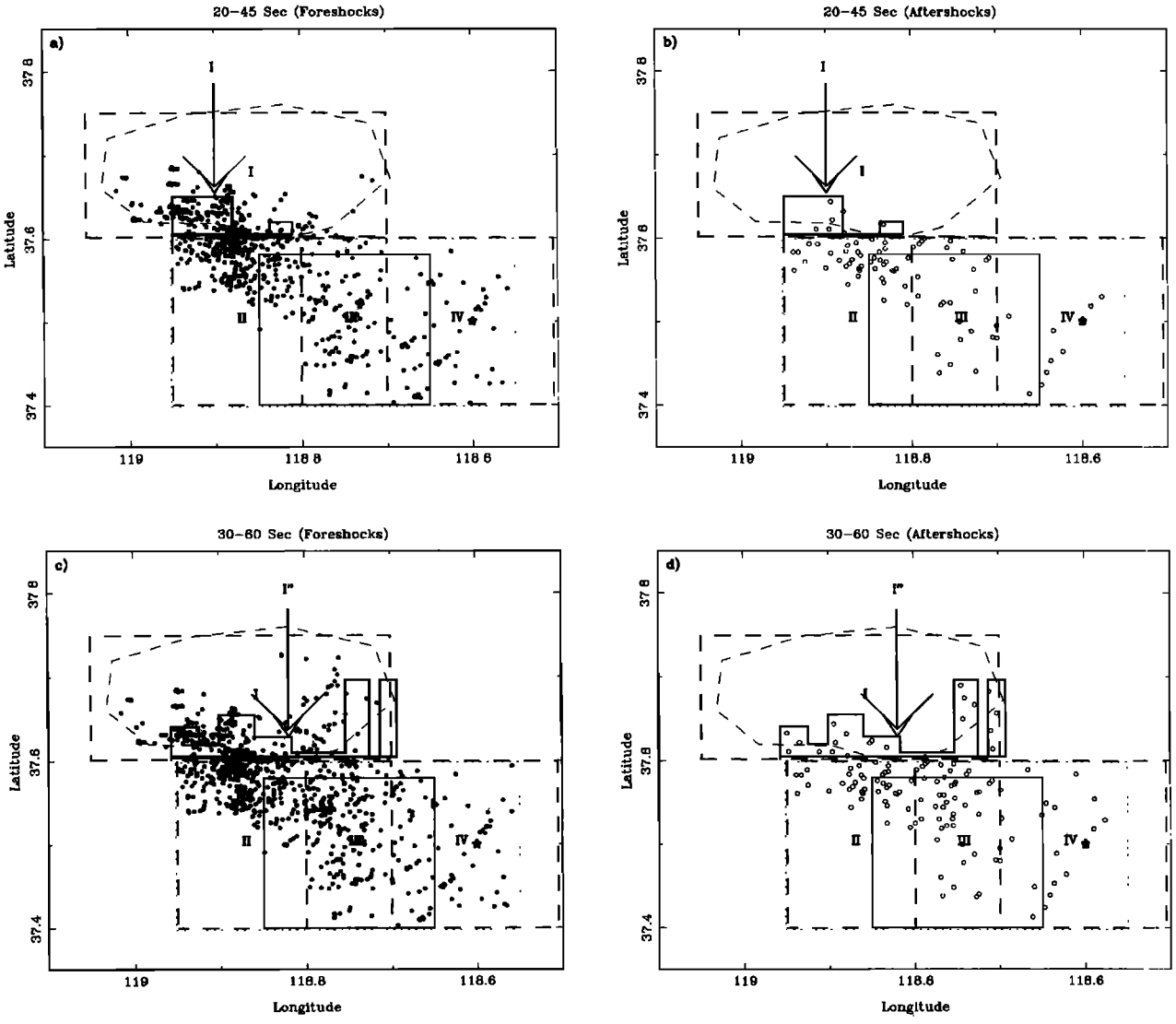

Fig. 3. Distribution of midpoints between sources and receivers for different time windows. Solid circles, foreshocks; open circles, aftershocks. Two subdivisions of region I enclosed by the solid lines north of 37.6°N are defined for the time windows 20-45 s (I') and 30-60 s (I"). Region I' is at the tip of the arrow in Figures 3a and 3b, and region I" is shown in Figures 3c and 3d.

similar to the coda Q. In other words, observations support the single-scattering model for the coda Q measurments. Even if the multiple scattering is significant, it is still convenient to use equation (1) as an empirical formula because the separation of intrinsic Q^{-1} and scattering Q^{-1} in the multiple-scattering case introduces a severe nonuniqueness in determining these parameters from the data. The use of equation (1) is justified even for the multiple-scattering cases as long as the time window is specified from which the coda is sampled. Taking the natural logarithm of both sides of equation (1) gives

$$\ln P(\omega|t) = \ln C(\omega) - 2 \ln t - \frac{\omega t}{Q_c} \qquad (2)$$

Because $C(\omega)$ is independent of time, $\ln C(\omega)$ can be treated as a constant in determining coda Q^{-1} for a given ω, and we have

$$\ln P(\omega|t) = \ln C(\omega) - 2 \ln t - \frac{\omega t}{Q_c} \qquad (3)$$

As in the work by Lee et al., [1986], we obtained coda Q^{-1} through the linear regression of equation (3) for five octave frequency bands centered at 1.5, 3, 6, 12, and 24 Hz, respectively, by taking a window size of 512 data samples and moving the window by 2.56 s and, at the same time, correcting for the instrument response.

The coda Q^{-1} obtained for a particular source and receiver is assigned to the midpoint of the source and receiver. We then group the coda Q^{-1} data according to the location of the midpoint

TABLE 2a. Mean Coda Q^{-1}, Number of Samples Used to Calculate Mean and Standard Error of the Mean for Five Frequency Bands With the Time Window 20-45 s in the Long Valley Caldera (Region I)

	Foreshock			Aftershock			Difference in (1/Q) Between Foreshocks and Aftershocks, %
Frequency Hz	(1/Q)x1000	Number of Samples	SEM	(1/Q)x1000	Number of Samples	SEM	
1.5	11.31	167	0.28	9.40	5	1.28	
3*	6.80	189	0.15	5.74	8	0.43	18
6	2.35	137	0.09	1.98	9	0.23	
12	0.79	112	0.03	0.69	8	0.10	
24	0.40	97	0.02	0.33	6	0.07	

SEM, Standard error of the mean.
*Significant difference.

TABLE 2b. Same as Table 2a for Time Window 30-60 s in Region I

	Foreshock			Aftershock			Difference in (1/Q) Between Foreshocks and Aftershocks, %
Frequency Hz	(1/Q)x1000	Number of Samples	SEM	(1/Q)x1000	Number of Samples	SEM	
1.5	11.59	99	0.36	9.40	5	1.28	
3*	6.84	105	0.18	5.74	8	0.43	17.5
6	2.28	81	0.10	1.98	9	0.23	
12	0.73	58	0.04	0.69	8	0.10	
24	0.36	50	0.02	0.33	6	0.03	

SEM, Standard error of the mean.
*Significant difference.

TABLE 2c. Same as Table 2a for Time Window 30-60 s in Region I

	Foreshock			Aftershock			Difference in (1/Q) Between Foreshocks and Aftershocks, %
Frequency Hz	(1/Q)x1000	Number of Samples	SEM	(1/Q)x1000	Number of Samples	SEM	
1.5	8.94	180	0.24	7.36	19	0.54	20
3*	4.04	194	0.11	2.99	19	0.22	30
6	1.32	168	0.04	1.36	15	0.15	
12*	0.71	171	0.02	0.57	18	0.04	22
24	0.39	107	0.02	0.36	11	0.03	

SEM, Standard error of the mean.
*Significant difference.

TABLE 2d. Same as Table 2a for Time Window 30-60 s in Region I''

	Foreshock			Aftershock			Difference in (1/Q) Between Foreshocks and Aftershocks, %
Frequency Hz	(1/Q)x1000	Number of Samples	SEM	(1/Q)x1000	Number of Samples	SEM	
1.5	8.92	125	0.29	7.36	19	0.54	19
3*	3.80	126	0.11	2.99	19	0.22	24
6	1.31	107	0.04	1.36	15	0.15	
12*	0.70	110	0.03	0.57	18	0.04	20
24	0.39	71	0.02	0.36	11	0.03	

SEM, Standard error of the mean.
*Significant difference.

TABLE 3. Same as Table 2a for Time Window 20-45 s in Region II

	Foreshock			Aftershock			Difference in (1/Q) Between Foreshocks and Aftershocks, %
Frequency Hz	(1/Q)x1000	Number of Samples	SEM	(1/Q)x1000	Number of Samples	SEM	
1.5	9.47	144	0.26	10.57	29	0.70	
3*	5.29	181	0.13	6.71	27	0.35	24
6*	1.58	145	0.05	2.19	32	0.19	32
12	0.76	130	0.03	0.78	31	0.06	
24	0.44	148	0.02	0.46	31	0.05	

SEM, Standard error of the mean.
*Significant difference.

TABLE 4a. Same as Table 2a for Time Window 20-45 s in Region III

	Foreshock			Aftershock			Difference in (1/Q) Between Foreshocks and Aftershocks, %
Frequency Hz	(1/Q)x1000	Number of Samples	SEM	(1/Q)x1000	Number of Samples	SEM	
1.5	9.38	58	0.45	11.50	17	1.77	
3	4.72	73	0.27	5.35	15	0.39	
6*	1.90	63	0.09	2.55	13	0.22	29
12	0.81	73	0.03	0.80	16	0.05	
24*	0.41	73	0.02	0.56	15	0.04	31

SEM, Standard error of the mean.
*Significant difference.

TABLE 4b. Same as Table 2a for Time Window 30-60 s in Region III

	Foreshock			Aftershock			Difference in (1/Q) Between Foreshocks and Aftershocks, %
Frequency Hz	(1/Q)x1000	Number of Samples	SEM	(1/Q)x1000	Number of Samples	SEM	
1.5	7.52	103	0.27	7.66	31	0.45	
3	3.36	124	0.15	3.78	30	0.38	
6*	1.33	114	0.07	1.09	21	0.07	20
12*	0.74	151	0.04	0.58	32	0.03	24
24	0.41	125	0.01	0.38	33	0.03	

SEM, Standard error of the mean.
*Significant difference.

TABLE 5. Same as Table 2a for Time Window 20-45 s in Region IV

	Foreshock			Aftershock			Difference in (1/Q) Between Foreshocks and Aftershocks, %
Frequency Hz	(1/Q)x1000	Number of Samples	SEM	(1/Q)x1000	Number of Samples	SEM	
1.5	8.11	43	0.43	8.37	6	1.36	
3*	4.68	58	0.19	5.63	6	0.29	19
6	2.01	46	0.12	1.40	2	0.10	
12	0.86	52	0.03	0.70	3	0.25	
24	0.44	50	0.02	0.53	7	0.15	

SEM, Standard error of the mean.
*Significant difference.

TABLE 6a. Same as Table 2a for Time Window 20-45 s in Region S

	Foreshock			Aftershock			Difference in (1/Q) Between Foreshocks and Aftershocks, %
Frequency Hz	(1/Q)x1000	Number of Samples	SEM	(1/Q)x1000	Number of Samples	SEM	
1.5	8.86	100	0.27	11.27	28	1.23	
3*	4.73	125	0.17	6.02	21	0.44	24
6	1.82	111	0.07	2.22	20	0.20	
12	0.79	127	0.02	0.71	23	0.05	
24	0.43	127	0.02	0.52	27	0.05	

SEM, Standard error of the mean.
*Significant difference.

TABLE 6b. Same as Table 2a for Time Window 30-60 s in Region S

	Foreshock			Aftershock			Difference in (1/Q) Between Foreshocks and Aftershocks, %
Frequency Hz	(1/Q)x1000	Number of Samples	SEM	(1/Q)x1000	Number of Samples	SEM	
1.5	7.60	142	0.24	7.32	37	0.37	
3	3.32	184	0.13	3.16	32	0.19	
6*	1.29	163	0.05	1.04	24	0.06	21
12*	0.72	219	0.03	0.61	38	0.03	17
24	0.43	165	0.01	0.42	44	0.03	

SEM, Standard error of the mean.
*Significant difference.

TABLE 7a. Same as Table 2a for Time Window 20-45 s in Region T

	Foreshock			Aftershock			Difference in (1/Q) Between Foreshocks and Aftershocks, %
Frequency Hz	(1/Q)x1000	Number of Samples	SEM	(1/Q)x1000	Number of Samples	SEM	
1.5	9.21	240	0.21	10.62	52	0.71	
3*	5.04	307	0.11	6.15	48	0.25	20
6*	1.73	248	0.04	2.25	47	0.15	26
12	0.79	249	0.02	0.78	50	0.05	
24	0.43	268	0.01	0.58	53	0.04	

SEM, Standard error of the mean.
*Significant difference.

TABLE 7b. Same as Table 2a for Time Window 30-60 s in Region T

	Foreshock			Aftershock			Difference in (1/Q) Between Foreshocks and Aftershocks, %
Frequency Hz	(1/Q)x1000	Number of Samples	SEM	(1/Q)x1000	Number of Samples	SEM	
1.5	7.91	316	0.17	7.91	68	0.29	
3	3.31	365	0.08	3.53	62	0.21	
6	1.24	326	0.03	1.14	49	0.07	
12*	0.69	419	0.02	0.61	71	0.02	12.3
24	0.41	329	0.01	0.43	68	0.02	

SEM, Standard error of the mean.
*Significant difference.

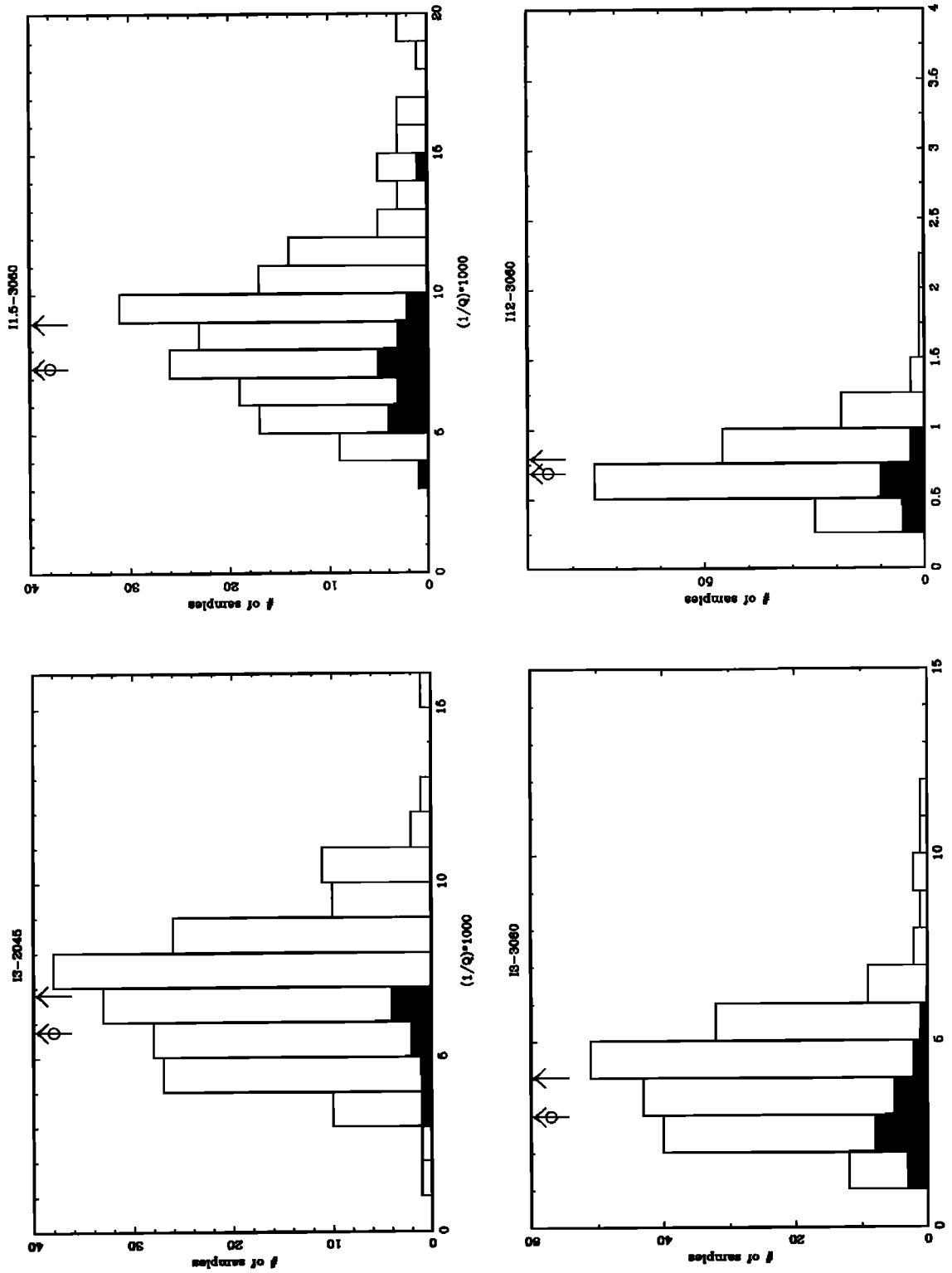

Fig. 4. Histograms of coda Q^{-1} for different frequency bands with statistically significant difference between foreshocks and aftershocks in the Long Valley caldera. Shaded area, aftershocks; unshaded area, foreshocks; arrow, mean for foreshocks; arrow with a superimposed circle, mean for aftershocks. The headings (e.g., 13-3060) give the region (I), the frequency (3 Hz) and the time window (30-60 s).

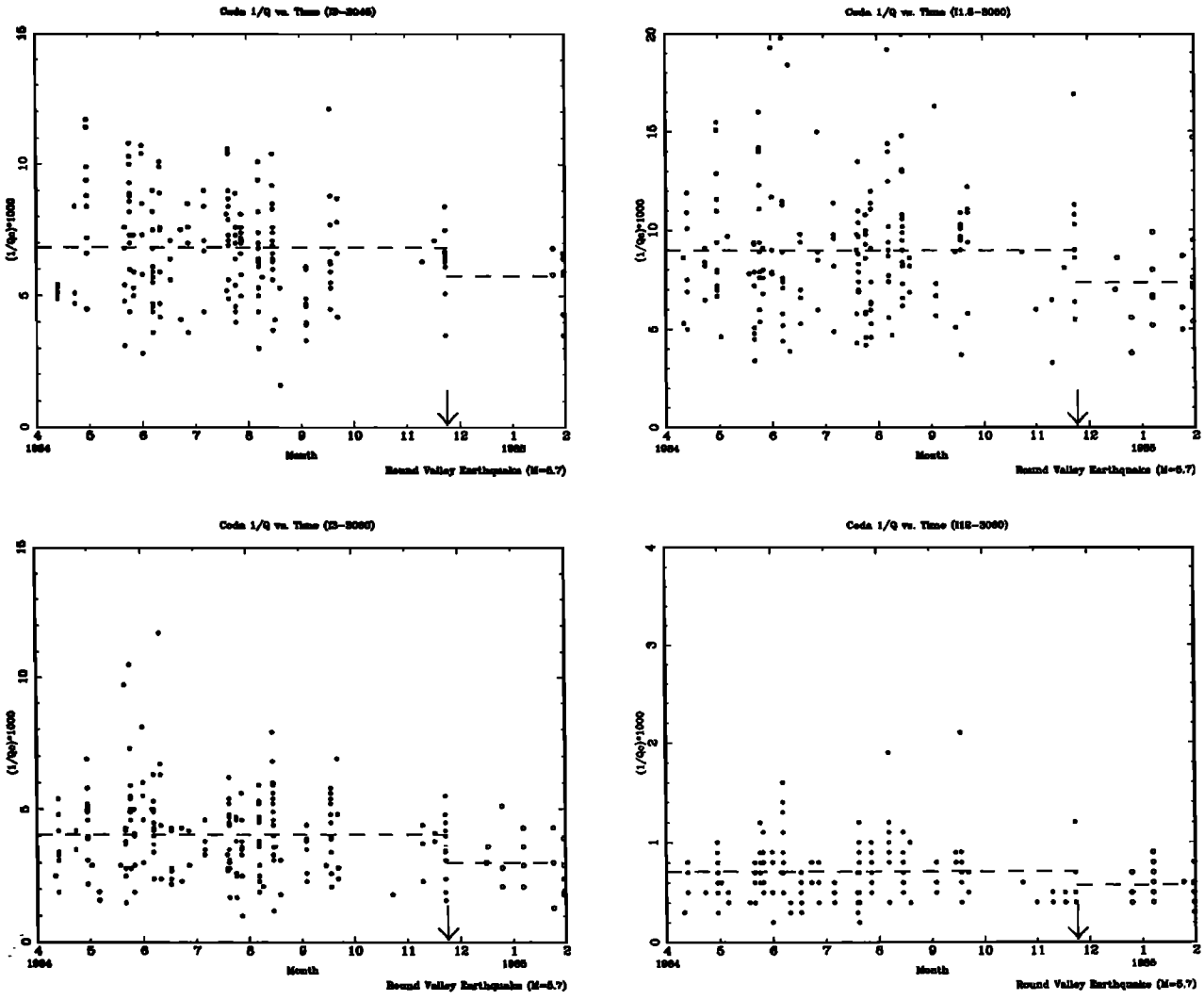

Fig. 5. Temporal variation of coda Q^{-1} for the data set shown in Figures 4. The arrow indicates the time of the main shock. The means for foreshocks and aftershocks are shown by dashed lines.

between source and receiver. Four separate regions (I, II, III, and IV with the area 15x40 km^2, 15x20 km^2, 10x20 km^2, 20x20 km^2, respectively) are grouped as shown by the dashed lines in Figuers 1, and two other areas S (solid line) and T (dotted line) are also considered. In order to reduce the bias due to different spatial coverage, we further subdivided region I into I' and I" as shown in Figure 3.

We apply a statistical test of significant to the differences between coda Q^{-1} before and after the main shock for each data set in the above defined regions. We also studied the significance of difference in coda Q^{-1} between different regions. In all the significance tests we used Q_c^{-1} instead of Q_c because the former more closely follows a Gaussian distribution than the latter.

We use the method of Fisher and Yates [1970] by forming the following statistics:

$$d = \frac{\overline{X}_1 - \overline{X}_2}{\sqrt{S_1^2 + S_1^2}} \qquad (4)$$

$$S_i = \frac{\sigma_i}{\sqrt{N_i - 1}} \qquad (5)$$

where

$\overline{X}_i$ mean of coda Q^{-1} for group i;
S_i standard error of the mean for group i;
σ_i standard error of all samples in group i;
N_i number of samples in group i.

This method is appropriate for the difference of two means for which the errors are due to different causes, so that estimates of variance cannot properly be pooled. This is exactly the case when coda Q^{-1} measurements were taken from a large number of seismograms. We consider the difference between two means to be significant when d in equation (4) exceeds the critical values for different sets of sampling numbers given by Sukhatme [1938] at the 95% confidence level. Otherwise, the difference is considered to be not significant. In other words, the critical values

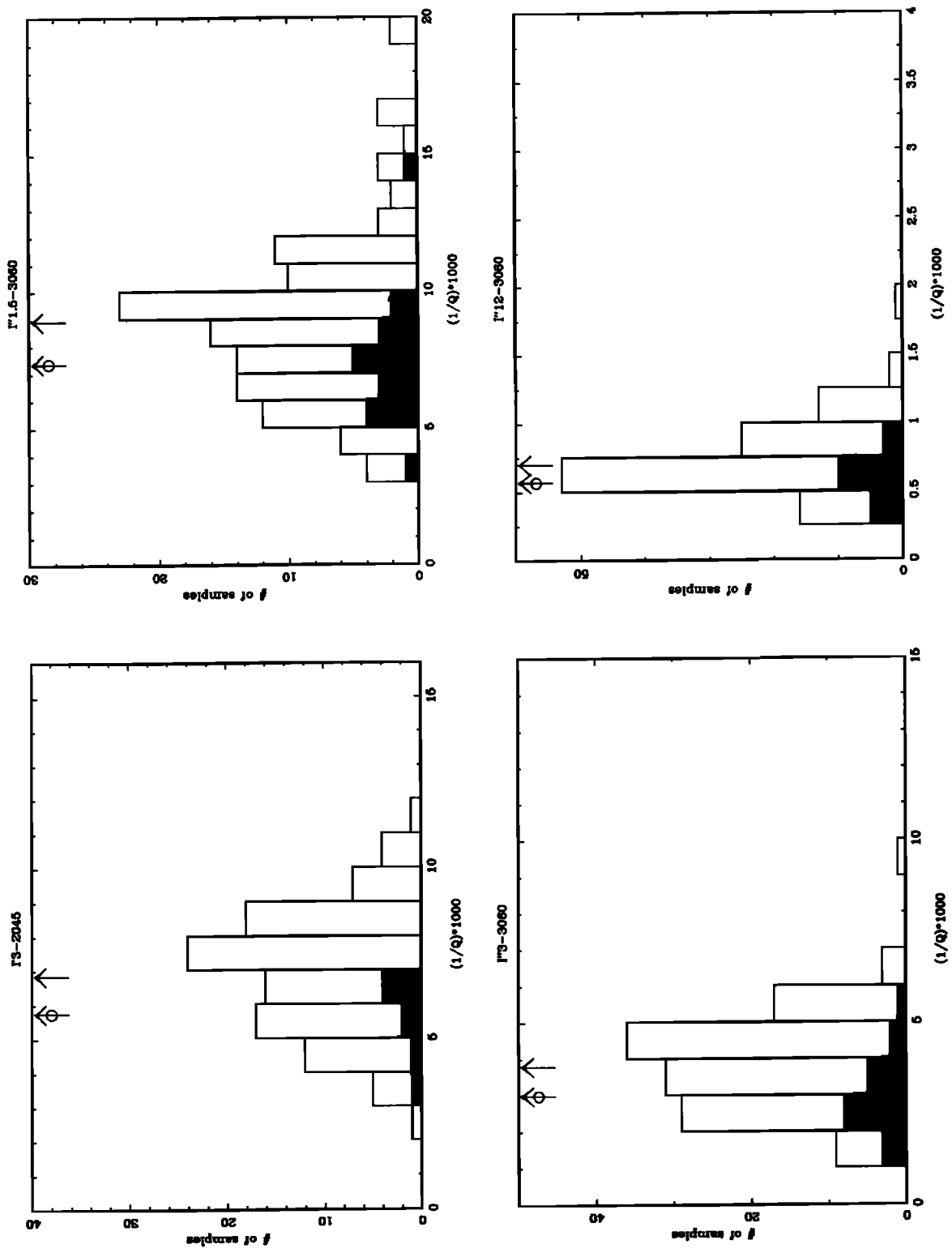

Fig. 6. Same as Figure 4 for foreshocks and aftershocks in regions I' and I".

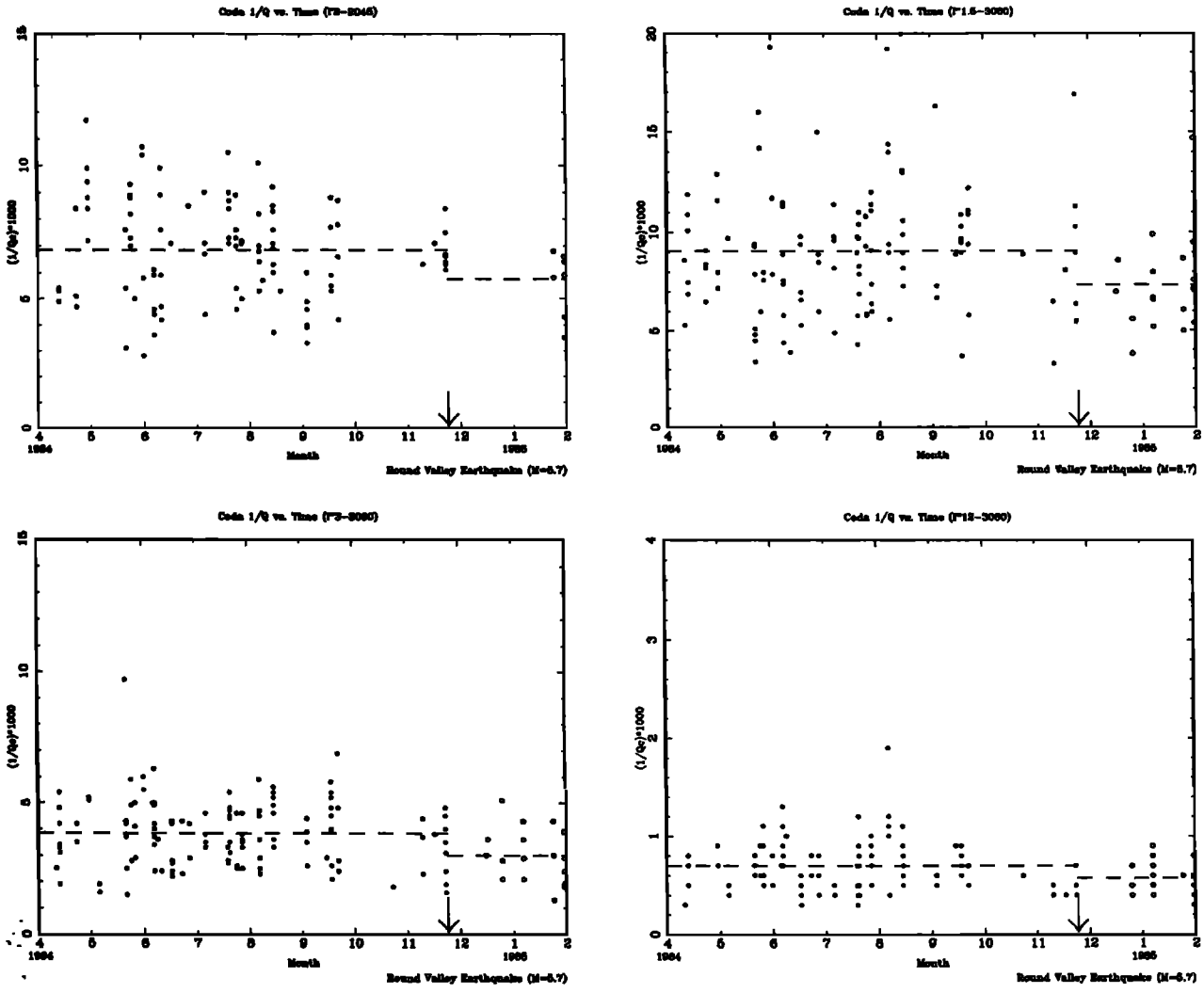

Fig. 7. Temporal variation of coda Q^{-1} for the data set shown in Figure 6.

of d depends not only on the sampled numbers of coda Q^{-1} for foreshocks and aftershocks but also varies as the scale factors (θ), where

$$\tan \theta = \frac{S_1}{S_2} \qquad (6)$$

Consequently, these parameters control the critical value of d in equation (4) for each significance test. Tables 2a-7b list these parameters in detail when the difference is significant.

Results

Most of our earthquakes (at least 85%) occurred in regions II, III, and IV, with many clustered south of the Long Valley caldera and northwest of Bishop (regions II and IV). Figure 3 shows the distribution of midpoints for foreshocks and aftershocks for two different time windows. We see that the midpoint distributions are nearly the same for data from both foreshocks and aftershocks.

Comparison of coda Q^{-1} between foreshocks and aftershocks is made for regions I, I', I", II, III, IV, S, and T in Tables 2a-7b where the mean coda Q^{-1}, the number of samples used to calculate the mean, and the standard error of the mean are shown for each frequency band. When the difference in the mean value between foreshock and aftershock is significant at the 95% level, the percentage change in coda Q^{-1} is shown in the last column.

The distributions of observed coda Q^{-1} in the form of histograms and temporal variation from April 1984 to January 1985 are shown in Figures 4-13 for the cases in which significant differences between foreshocks and aftershocks were found by the significance test. We found a consistent pattern of the change in coda Q^{-1}. The coda Q^{-1} increased after the main shock in regions II, III, and IV for the time window 20-45 s, but it decreased for all the windows in region I which was located farthest from the main shock epicenter. The change is 20-30% when significant. A similar

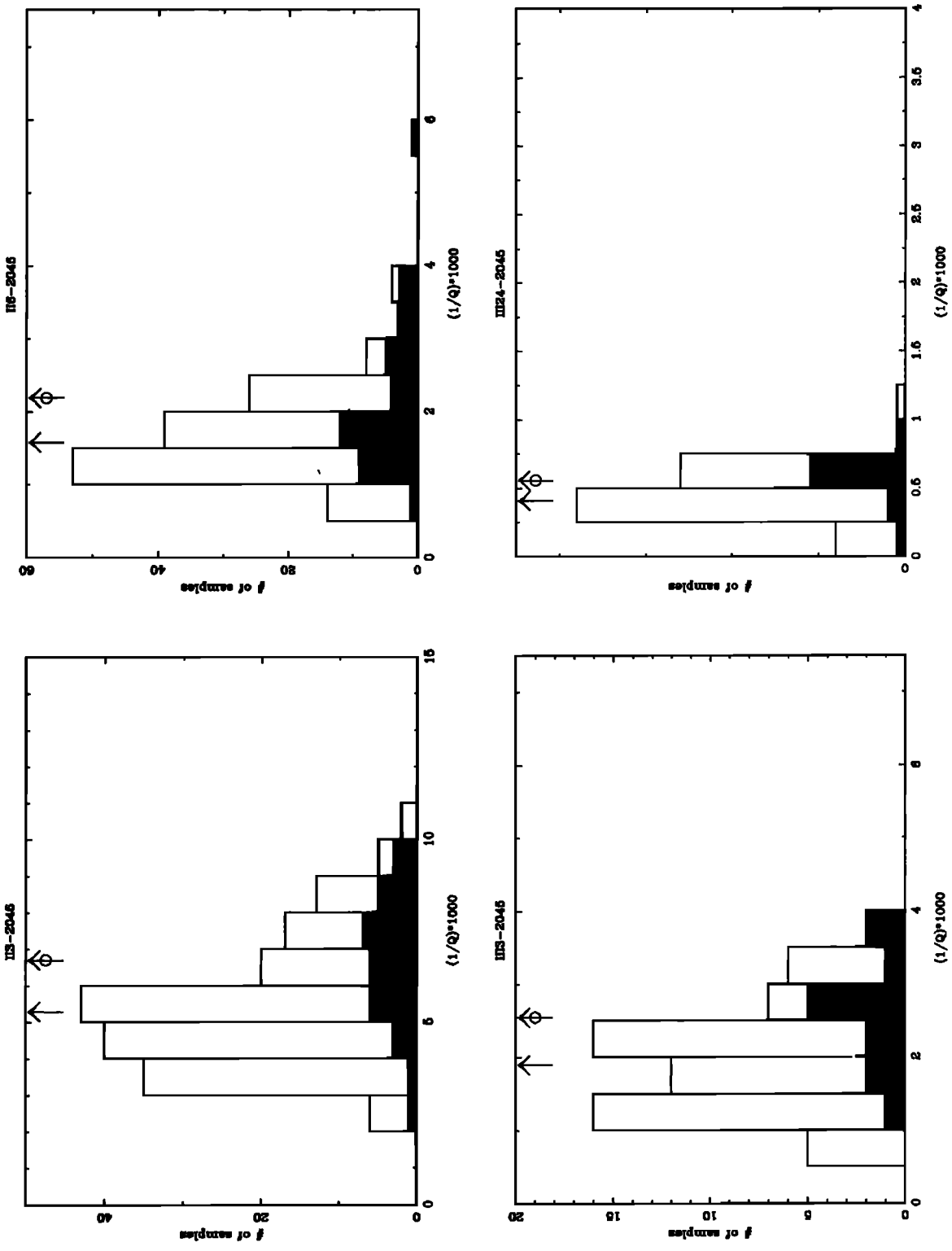
IIS-2045
# of samples
(1/Q)*1000
IIS-2045
# of samples
(1/Q)*1000
IIS-2045
# of samples
(1/Q)*1000
IIS24-2045
# of samples
(1/Q)*1000

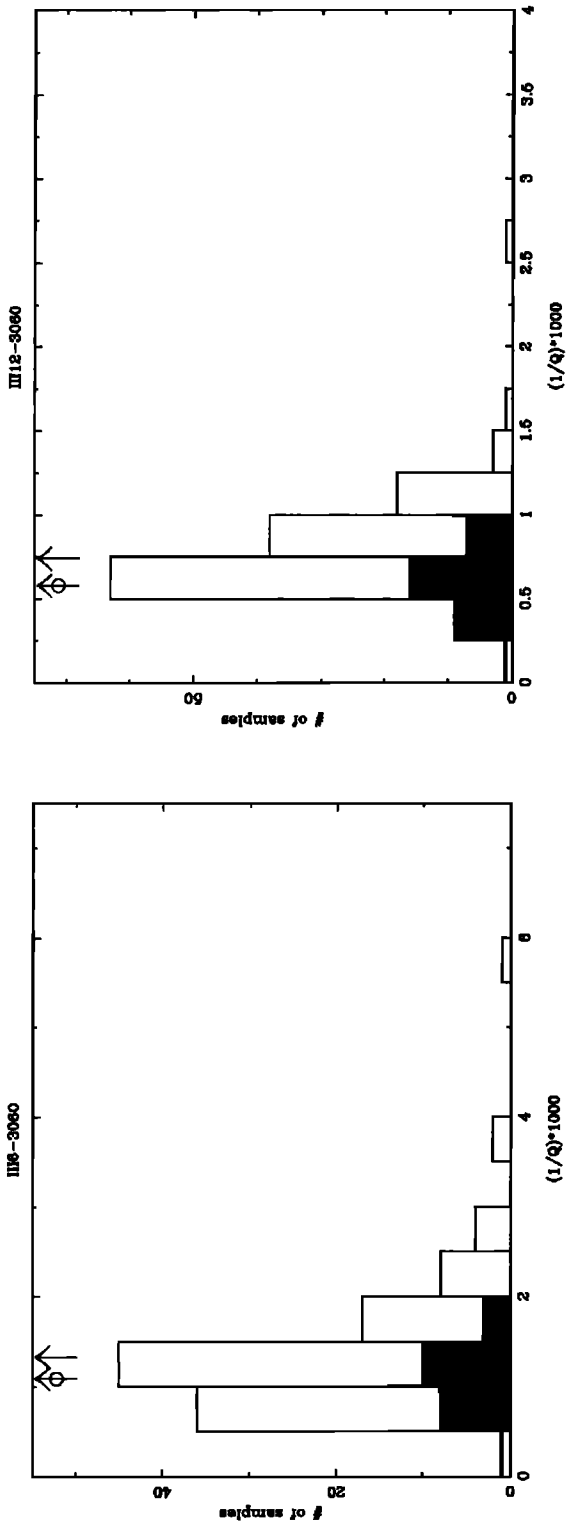

Fig. 8. Same as Figure 4 for foreshocks and aftershocks in regions II and III.

near-source increase of coda Q^{-1} after the occurrence of the main shock was also observed by Tsukuda [1985] for the Misasa earthquake (M=6.2) in Japan.

Contrary to what was found for the time window 20-45 s, aftershocks showed lower coda Q^{-1} than foreshocks in region III for the time window 30-60 s. The results for region II for the time window 30-60 s are inconclusive because none of the differences were significant.

In order to test the reliability of patterns of change in coda Q^{-1} we regrouped the data in regions II, III, and IV into regions S (area enclosed by solid line in Figure 1) and T (area enclosed by dotted line in Figure 1 encompassing areas II, III, and IV). Regions S and T exhibit significant differences for both windows (Tables 6a-7b). We found that aftershocks showed lower coda Q^{-1} than foreshocks for the time window 30-60 s for both S and T. This result is in good agreement with that measured from region III for time window 30-60 s. The difference was about 20% for area S and about 10% for area T. On the other hand, for both S and T, aftershocks showed higher coda Q^{-1} than foreshocks for the time window 20-45 s which is in agreement with the result obtained from this time window for areas II, III, and IV.

In region I (Long Valley caldera), aftershocks showed lower coda Q^{-1} than foreshocks for both time windows (Figures 4 and 5). This result is in agreement with the above result for areas in S and T for time window 30-60 s and the results obtained in most other reported cases [Gusev and Lemzikov, 1985; Novelo-Casanova et al., 1985; Jin and Aki, 1986; Sato, 1986]. Finally, we found that there was a significant spatial difference in coda Q^{-1} before the main shock between region I (Long Valley caldera) and region T when the same significance test was applied. Surprisingly, this difference, however, disappeared after the main shock. More precisely, the coda Q^{-1} at 3 Hz for time window 20-45 s was 6.8×10^{-3} in region I (Table 2a) and 5.0×10^{-3} in region I and 6.2×10^{-3} in region T for aftershocks. A significant spatial difference of about 30% not only disappeared but changed sign between Long Valley caldera and region T. We note that the temporal variation of coda Q^{-1} (e.g., 20-45 s) is comparable to its spatial variation.

Region I (Long Valley caldera) clearly shows higher coda Q^{-1} for foreshocks than aftershocks. To make sure this difference is not due to differences in the spatial distribution of midpoints over the central part of the caldera as shown in Figure 3, we have further defined regions I' and I" within which midpoint distributions of foreshocks and aftershocks are similar for the 20-45 s and 30-60 s windows, respectively. A comparison between aftershocks and foreshocks for regions I' and I" is shown in Figures 6 and 7 and, again, is consistent with the result obtained from region I. This excludes the possibility that greater coverage of midpoints over the central part of the caldera in region I by foreshocks than aftershocks is responsible for the result of temporal variation in coda Q^{-1}. It is also interesting to note that the spatial variation in coda Q^{-1} has the same magnitude as that of temporal variation for several regions. For example, compare regions I' and II for the 20-45 s window at

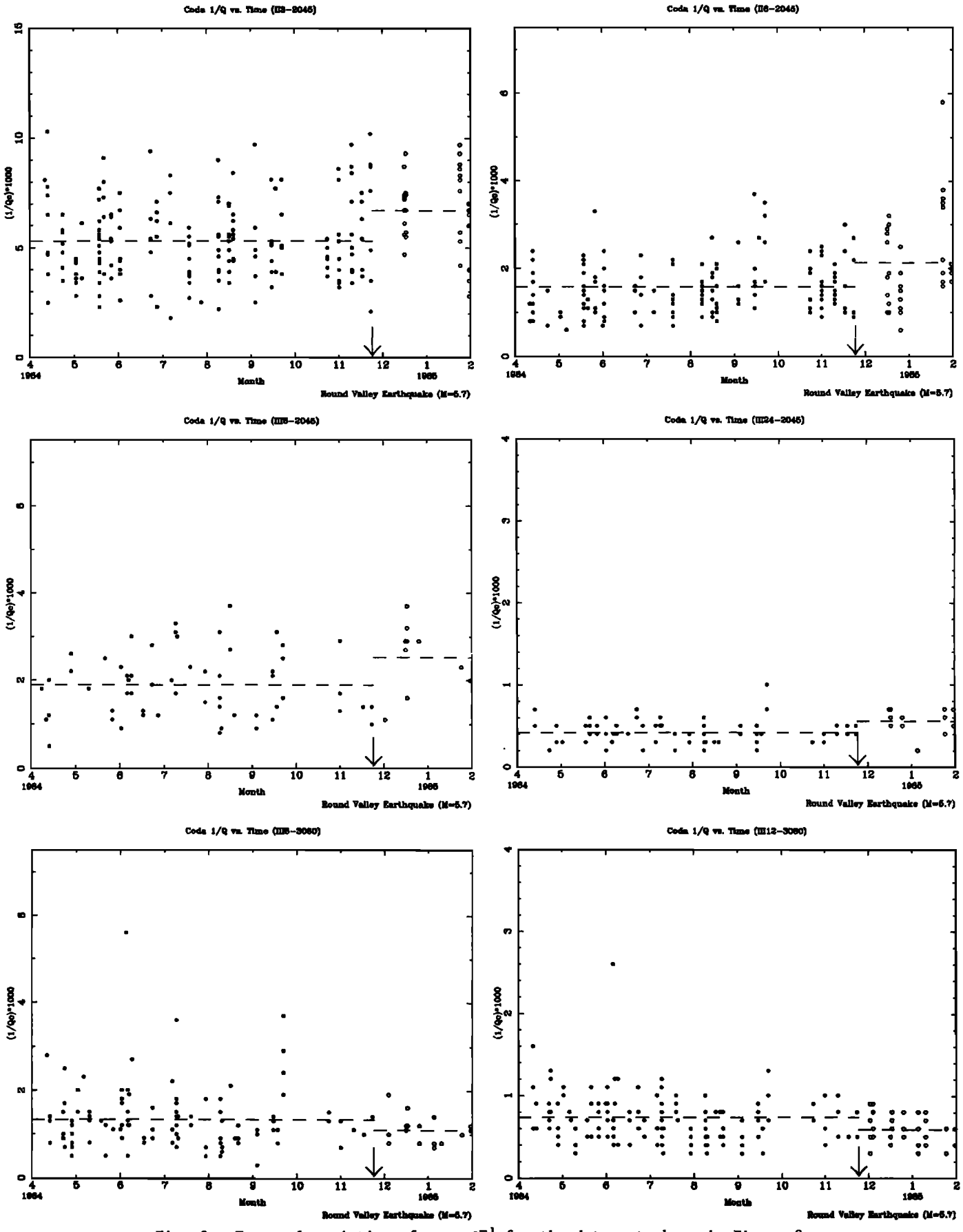

Fig. 9. Temporal variation of coda Q^{-1} for the data set shown in Figure 8.

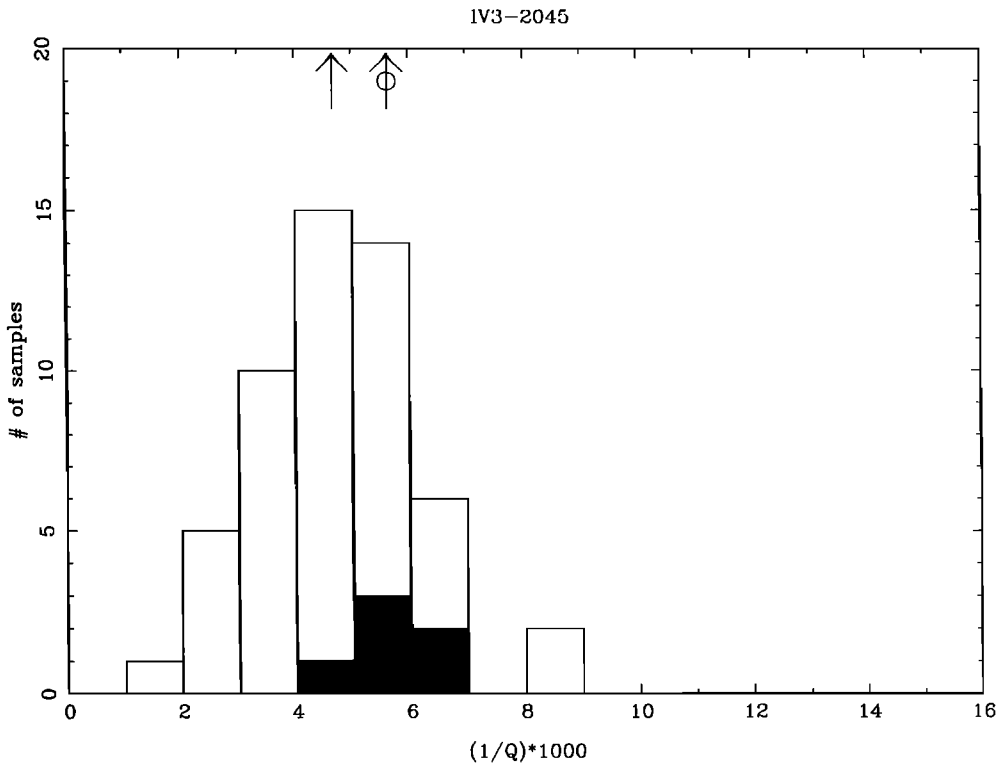

Fig. 10. Same as Figure 3 for foreshocks and aftershocks in region IV.

3Hz. Region I' shows higher coda Q^{-1} for foreshocks than region II and lower coda Q^{-1} for aftershocks than region II (Tables 2b and 3a). The decrease of coda Q^{-1} with time for region I' and the increase for region II are significant. A similar pattern of change in coda Q^{-1} can be seen between regions I" and T for the time window 30-60 s (Tables 2d and 7b).

Discussion and Conclusion

From the results which passed the significance test at 95% level we found that coda Q^{-1} for aftershocks is higher than that for foreshocks in the area close to the epicenter of the main shock but lower than that for foreshocks in the area farther away from the epicenter. This pattern of change can be easily seen from Figures 8-13. This is a reminiscent of Mogi's doughnut pattern of precursory seismicity [Kanamori, 1981; Mogi, 1985], in which an area of quiescence is surrounded by an active zone. In Mogi's model an earthquake will induce cracks or otherwise make the surrounding medium less competent, which will in turn elevate the coda Q^{-1}. Therefore we may expect that the area of quiescence has low coda Q^{-1} and the active

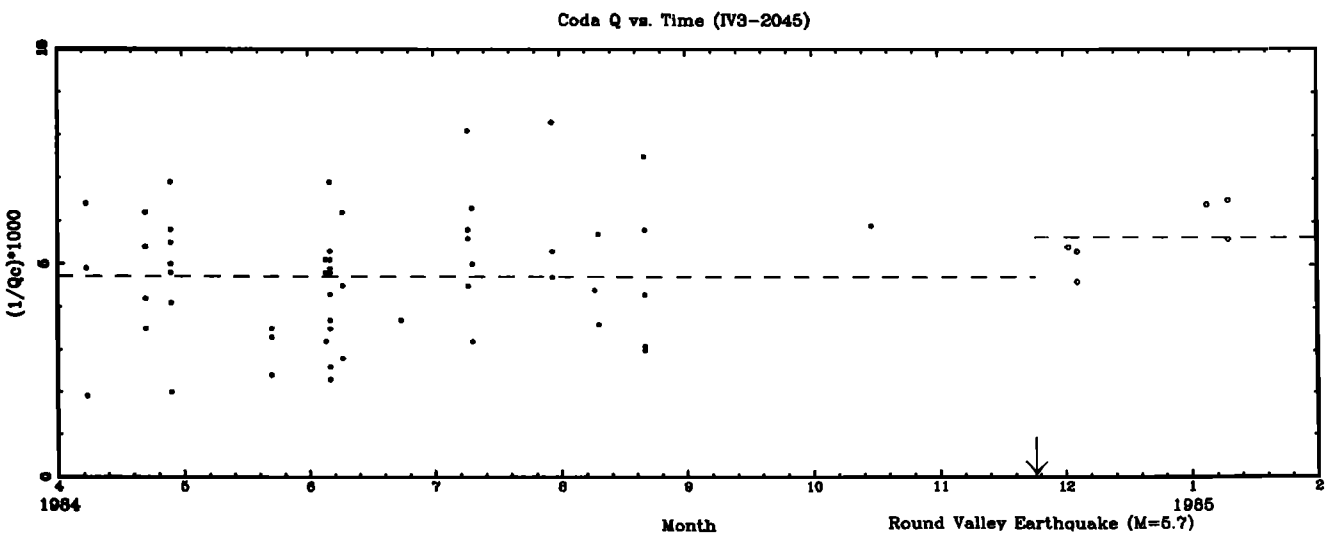

Fig. 11. Temporal variation of coda Q^{-1} for the data set shown in Figure 10.

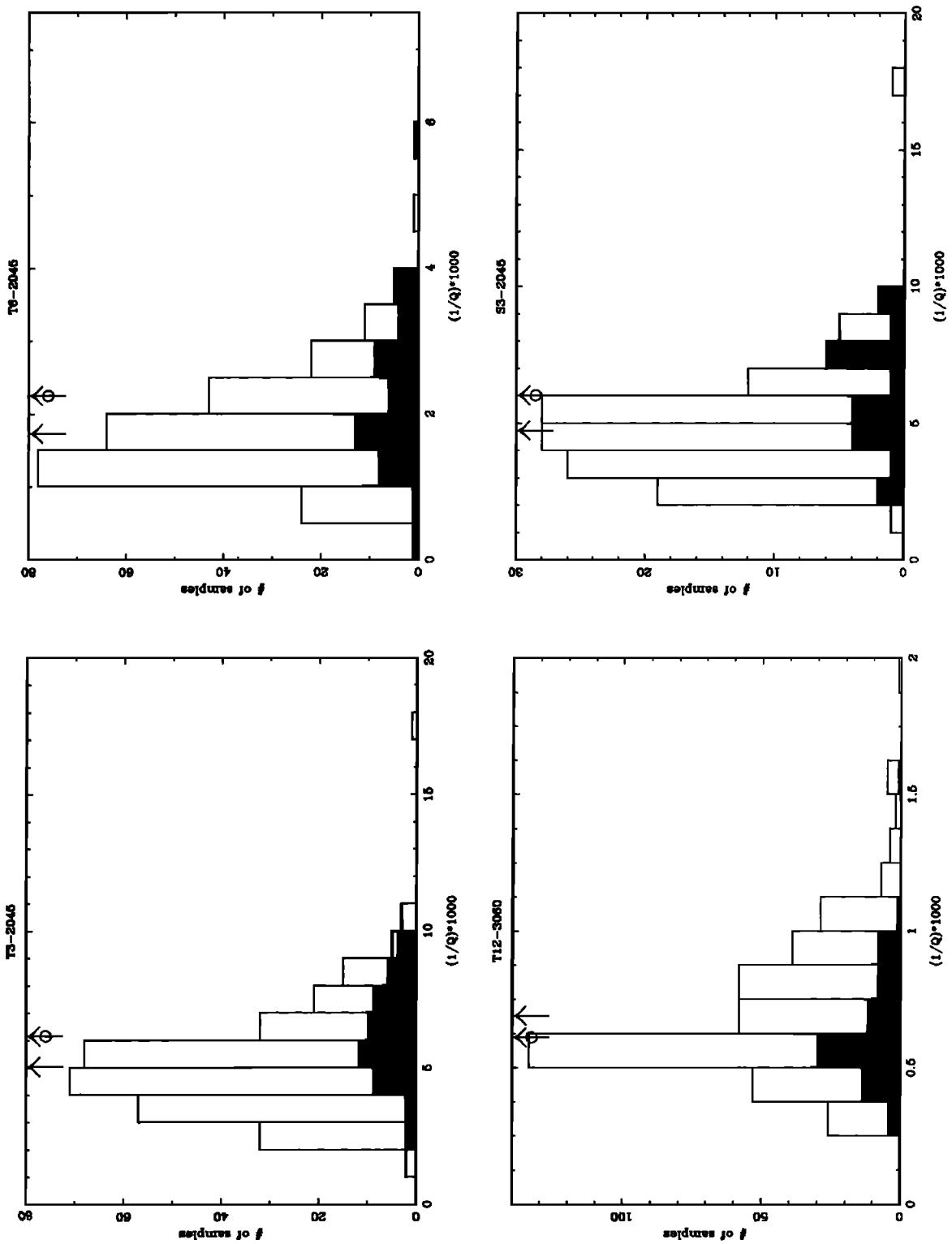
T3-2045
# of samples
(1/Q)*1000
S3-2045
# of samples
(1/Q)*1000
T3-2045
# of samples
(1/Q)*1000
T12-3060
# of samples
(1/Q)*1000

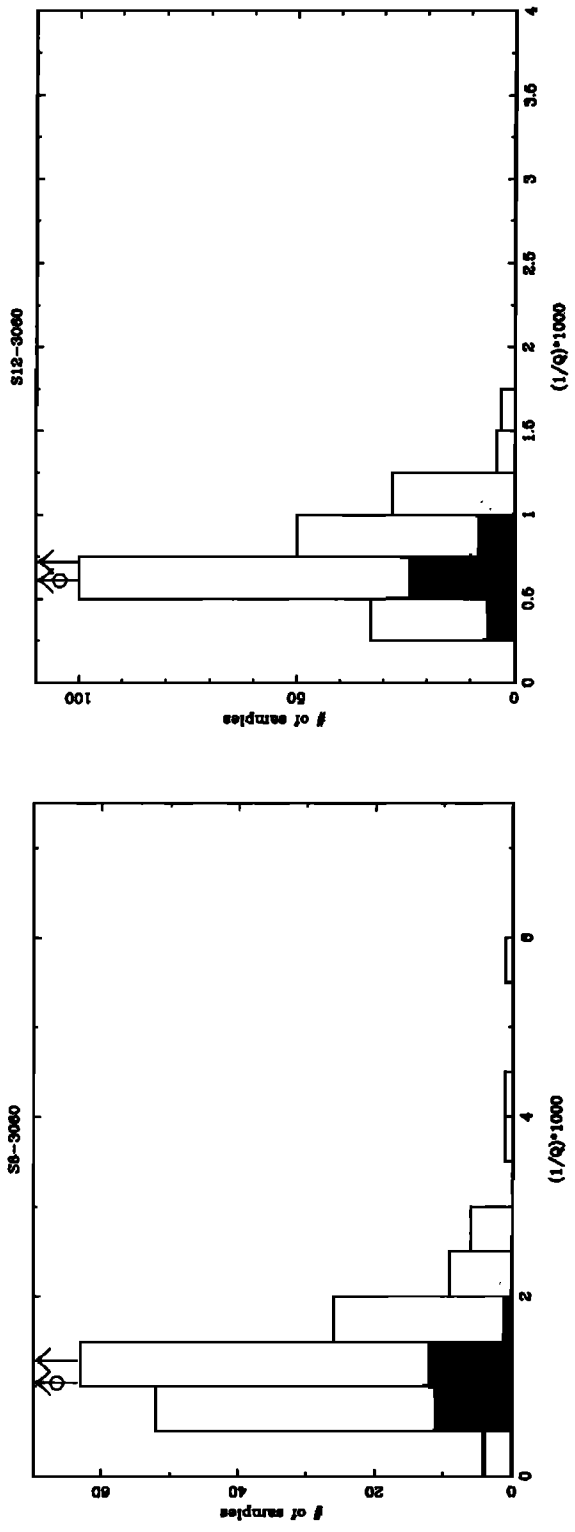

Fig. 12. Same as Figure 4 for foreshocks and aftershocks in regions T and S.

zone has high coda Q^{-1} before the main shock. After the main shock, however, the region of aftershocks in the immediate vicinity of the main shock fault zone becomes high in coda Q^{-1}, and the active zone of the doughnut may become quiet and low in coda Q^{-1}. Thus the spatial and temporal pattern of coda Q^{-1} variation observed in the Mammoth Lakes-Bishop area is in harmony with the general idea developed for the seismicity precursor, although we do not have obvious seismicity precursors in the case of the Round Valley earthquake.

We also found that the value of coda Q^{-1} obtained by a single measurement shows a large variance as evidenced in histograms of Figures 4, 6, 8, 10, and 12. From these histograms we can not find a simple geographic variations in coda Q^{-1} values. The large variance required a large number of measurments for detecting small difference in coda Q^{-1} as shown in Table 2a-7b. The observed large variation may be attributed to the nature of scattering sources in the lithosphere. Probably a small number of strong scatterers dominate the coda in seismically active zone. We are planning a Monte Carlo experiment to simulate coda to study the cause of the large variance in observed coda Q^{-1}.

In conclusion, the doughnut model which was invoked for explaining precursory seismicity patterns appears to explain, at least for the Mammoth Lakes-Bishop area, the observed coda Q^{-1} variation associated with the Round Valley earthquake. It also helps to reconcile conflicting results reported in published case studies of the coda Q^{-1} precursor. In this study we found a result similar to that of Tsukuda [1985] for areas near to the main shock location and sampled by short lapse time. On the contrary, for those regions which are farther away from the main shock epicenter and sampled by long lapse time, our result is consistent with these reports from other published cases.

We see clearly and consistently that coda Q^{-1} decreased toward the end for both 20-45 s and 30-60 s in region I and increased toward the end for 20-45 s but not for 30-60 s in regions II, III, and IV. It is, however, difficult to tell when the change occurred because of large variance of data. In this case, the only possibility was hypothesis testing. We chose the null hypothesis that coda Q^{-1} in the 8 months before the earthquake was equal to the coda Q^{-1} in the 2 months following the earthquake. The hypothesis was rejected by the significant test.

A major puzzle, however, remains about coda Q^{-1} if this observed temporal change is real. The observed temporal change suggests that heterogeneities responsible for the scattering and attenuation of coda waves are crack-related because only thin cracks can respond sensitively to a small stress change. At depths where we presume that the scatterers exist, these cracks must be kept open by high pore pressure. Since fluid will have finite viscosity, intrinsic Q of S waves will be low. From the results shown above, the coda Q^{-1} is always less than 0.001 for frequencies higher than 10 Hz. Multiple scattering [e.g., Gao et al., 1983; Wu and Aki, 1985; Frankel and Clayton, 1986] can cause apparent low coda Q^{-1} in the result

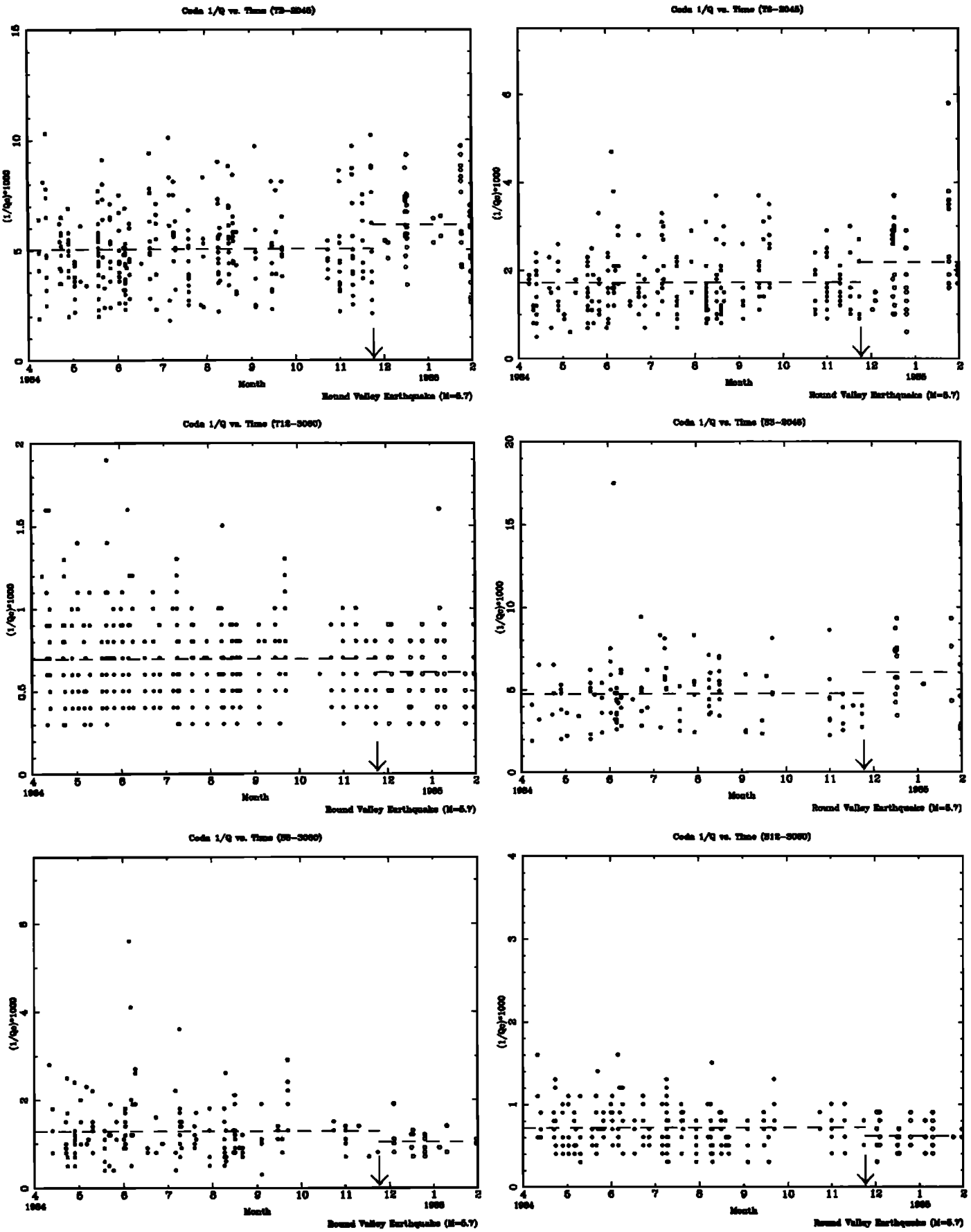

Fig. 13. Temporal variation of coda Q_{-1} for the data set shown in Figure 12.

obtained by the coda method, but the agreement between coda Q^{-1} measured using single-scattering model and Q^{-1} of S waves measured by an independent method [e.g., Aki 1980a] is usually excellent for high frequencies and short lapse times. Of course, the separation of intrinsic and scattering Q^{-1} may provide some clue to the above problem. It is, however, difficult in practice to apply any multiple-scattering models to actual data because the separation of intrinsic and scattering Q^{-1} introduces a severe nonuniqueness in determining these parameters from the data.

Acknowledgments. We thank Steve Roecker, Bruce Julian, Caryl Michaelson, and James W. Dewey for their careful readings of the manuscript and valuable comments. An anonymous reviewer is also appreciated for suggesting the improvements of the figures. This work was supports by U.S. Geological Survey grants 14-08-0001-A-0036 and 14-08-0001-G-1195.

References

Aki, K., Analysis of the seismic coda of local earthquakes as scattered waves, J. Geophys. Res., 74, 615-631, 1969.

Aki, K., Attenuation of shear-waves in the lithosphere for the frequencies from 0.05 to 25 Hz. Phys. Earth Planet. Inter., 21, 50-60, 1980a.

Aki, K., Scattering and attenuation of shear waves in the lithosphere, J. Geophys. Res., 85, 6496-6504, 1980b.

Aki, K., and B. Chouet, Origin of coda waves: Source, attenuation and scattering effects, J. Geophys. Res., 80, 3322-3342, 1975.

Chouet, B., Temporal variation in the attenuation of earthquake coda near Stone Canyon, California, Geophys. Res. Lett., 6, 143-146, 1979.

Fisher, R. A., and F. Yates, Statistical tables for Biological Agricultural and Medical Research, pp. 1-146, Hafner, 1970, Darien, Conn.

Frankel, A., and R. W. Clayton, Finite difference simulations of seismic scattering: Implications for the propagation of short-period seismic waves in the crust and models of crustal heterogeneity, J. Geophys. Res., 91, 6465-6489, 1986.

Gao, L. S., L. C. Lee, N. N. Biswas, and K. Aki, Comparison of the effects between single and multiple scattering on coda waves for local earthquakes, Bull. Seismol. Soc. Am.., 73, 377-389, 1983.

Gusev, A. A., and V. K. Lemzikov, Properties of scattered elastic waves in the lithosphere of Kamchatka: Parameters and temporal variation, Tectonophysics, 112, 137-153, 1985.

Jin, A., On the duration of coda waves and the back-scattering coefficient, in Proceedings of the Symposium on Seismology in China, Seismological Publishing House, Shanghai, People's Republic of China, 1981.

Jin, A., and K. Aki, Temporal change in coda Q before the Tangshan earthquake of 1976 and the Haicheng earthquake of 1975, J. Geophys. Res., 91, 665-673, 1986.

Johnson, P., and S. W. Stewart, Caltech-USGS seismic processing system (CUSP): User documentation, U.S. Geol. Surv. Open-File Rep., in press, 1986.

Julian, B. R., and S. Sipkin, Earthquake processes in the Long Valley area, California, J. Geophys. Res., 90, 11,155-11,169, 1985.

Kanamori, H., The nature of seismicity patterns before large earthquakes, in Earthquake Prediction, An International Review, Maurice Ewing Ser., vol. 4, edited by D. W. Simpson and P. G. Richards, pp. 1-20, AGU, Washington, D.C., 1981.

Kopnichev, Y. F., Models for the formation of the coda of the longitudinal wave, (Dokl. Akad. Nauk. SSSR, Engl. Transl.), 234, 13-15, 1977.

Lee, W. H. K., K. Aki, B. Chouet, P. Johnson, S. Marks, J. T. Newberry, A. S. Ryall, S. W. Stewart, and D. M. Tottingham, A preliminary study of coda Q in California and Nevada, Bull. Seismol. Soc. Am., in press, 1986.

Mogi, K., Earthquake Prediction, pp. 1-355, Academic Press, 1985, Orlando, Florida.

Novelo-Casanova, D. A., E. Berg, V. Hsu, and C. E. Helsley, Time-space variation seismic S-wave coda attenuation (Q^{-1}) and magnitude distribution for the Pelatan earthquake, Geophys. Res. Lett., 12, 789-792, 1985.

Rautian, T. G., and V. I. Khalturin, The use of coda for determination of the earthquake source spectrum, Bull. Seismol. Soc. Am., 68, 923-940, 1978.

Rhea, S., Q determined from local earthquakes in the South Carolina coastal plain, Bull. Seism. Soc. Am., 74, 2257-2268, 1984.

Roecker, S. W., B. Tucker, J. King, and D. Hatzfeld, Estimates of Q in Central Asia as a function of frequency and depth using the coda of locally recorded earthquakes. Bull. Seismol. Soc. Am., 72, 129-149, 1982.

Sato, H., Energy propagation including scattering effects, single isotrophic approximation, J. Phys. Earth, 25, 27-41, 1977.

Sato, H., Attenuation and envelope formation of three-component seismograms of small local earthquakes in randomly inhomogeneous lithosphere, J. Geophys. Res., 89, 1221-1241, 1984.

Sato, H., Temporal change in attenuation intensity before and after the eastern Yamanashi earthquake of 1983 in central Japan, J. Geophys. Res., 91, 2049-2061, 1986.

Scholz, C. H., L. R. Sykes, and Y. P. Aggrawal, Earthquake prediction: A physical basis, Science, 181, 803-810, 1973.

Sukhatme, P. V., On fisher and Behren's test of significance for the difference in means of two normal samples, Sankhya, 4, 39-48, 1938.

Tsukuda, T., Coda Q before and after a medium-scale earthquake, paper presented at the 23rd General Assembly, Int. Assoc. of Seismol. and Phys. of the Earth's Inter., Tokyo, Aug. 1985.

Tsujiura, M., Spectral analysis of the coda waves from local earthquakes, Bull. Earthquake Res. Inst. Univ. Tokyo, 53, 1-48, 1978.

Wilson, M., M. Wyss, and R. Koyanagi, Temporal attenuation change in the Koae fault system, southern Hawaii, EOS, Trans. AGU, 64, 761, 1983.

Wu, R. S., Seismic wave scattering and the small

scale inhomogeneities in the lithosphere, Ph.D. thesis, Mass. Inst. of Technol., Cambridge, 1984.

Wu, R. S., and K. Aki, Elastic wave scattering by a random medium and the small-scale inhomogeneities in the lithosphere, J. Geophys. Res., 90, 10,261-10,273, 1985.

Wyss, M., Precursors to large earthquakes, Earthquake Predict. Res., 3, 519-543, 1985.

J. Y. Peng and K. Aki, Department of Geological Sciences, University of Southern California, University Park, Los Angeles, CA 90089.

B. Chouet, P. Johnson, W. H. K. Lee, S. Marks, S. W. Stewart, and D. M. Tottingham, U. S. Geological Survey, 345 Middlefxield Road, MS 77, Menlo Park, CA 94025.

J. T. Newberry, Sierra Geophysics, Inc., P.O. Box 3886, Seattle, WA 98124.

A. S. Ryall, Center for Seismic Studies, 1300 North 17th Street, Suite 1450, Arlington, VA 22209.

(Received April 18, 1986;
revised October 10, 1986;
accepted October 13, 1986.)